Crystal structure and catalytic mechanism of the LPS 3-*O*-deacylase PagL from *Pseudomonas aeruginosa*

Lucy Rutten*†, Jeroen Geurtsen†‡§, Wietske Lambert*, Jeroen J. M. Smolenaers*, Alexandre M. Bonvin¶, Alex de Haan‡, Peter van der Ley‡, Maarten R. Egmond‖, Piet Gros*, and Jan Tommassen§**

Departments of *Crystal and Structural Chemistry, ¶NMR Spectroscopy, and ‖Membrane Enzymology, Bijvoet Center for Biomolecular Research, and §Department of Molecular Microbiology, Utrecht University, Padualaan 8, 3584 CH, Utrecht, The Netherlands; and ‡Netherlands Vaccine Institute, P.O. Box 457, 3720 AL, Bilthoven, The Netherlands

Edited by Douglas C. Rees, California Institute of Technology, Pasadena, CA, and approved March 15, 2006 (received for review October 28, 2005)

Pathogenic Gram-negative bacteria can modify the lipid A portion of their lipopolysaccharide in response to environmental stimuli. 3-*O*-deacylation of lipid A by the outer membrane enzyme PagL modulates signaling through Toll-like receptor 4, leading to a reduced host immune response. We found that PagL is widely disseminated among Gram-negative bacteria. Only four residues are conserved: a Ser, His, Phe, and Asn residue. Here, we describe the crystal structure of PagL from *Pseudomonas aeruginosa* to 2.0-Å resolution. It consists of an eight-stranded β-barrel with the axis tilted by ≈30° with respect to the lipid bilayer. The structure reveals that PagL contains an active site with a Ser-His-Glu catalytic triad and an oxyanion hole that comprises the conserved Asn. The importance of active site residues was confirmed in mutagenesis studies. Although PagL is most likely active as a monomer, its active site architecture shows high resemblance to that of the dimeric 12-stranded outer membrane phospholipase A. Modeling of the substrate lipid X onto the active site reveals that the 3-*O*-acyl chain is accommodated in a hydrophobic groove perpendicular to the membrane plane. In addition, an aspartate makes a hydrogen bond with the hydroxyl group of the 3-*O*-acyl chain, probably providing specificity of PagL toward lipid A.

lipopolysaccharide | outer membrane protein | serine hydrolase

The outer membrane of Gram-negative bacteria functions as a permeability barrier that protects the bacteria against harmful compounds from the environment. It is an asymmetric bilayer with phospholipids and lipopolysaccharides (LPS) in the inner and outer leaflet, respectively. LPS contains three covalently linked domains: lipid A, the core, and the *O*-antigen (1). Lipid A forms the hydrophobic membrane anchor and is responsible for the endotoxic activity of LPS. In *Escherichia coli*, it consists of a 1,4′-bisphosphorylated β-1,6-linked glucosamine disaccharide, which is substituted with *R*-3-hydroxymyristic acid (3-OH C14) residues at positions 2, 3, 2′, and 3′ via ester or amide linkage. Secondary lauroyl and myristoyl groups substitute the hydroxyl group of 3-OH C14 at the 2′ and 3′ positions, respectively. The underlying mechanism for LPS toxicity is its recognition by the host Toll-like receptor 4–MD2 complex, resulting in a signaling cascade within the host cell. Signaling eventually leads to activation of the transcription factor NF-κB, which regulates the production of pro-inflammatory cytokines (reviewed in ref. 2).

Several Gram-negative bacteria, including *Salmonella enterica* serovar *typhimurium* (*S. typhimurium*), covalently modify their LPS in response to environmental stimuli. These modifications usually require the two-component regulatory system PhoP/PhoQ, which can be activated by antimicrobial peptides or repressed by high concentrations of divalent cations (3). The PhoP/PhoQ system activates or represses the expression of >40 genes, some of which are involved in antimicrobial peptide resistance. Two integral outer membrane enzymes, the PhoP/PhoQ-activated gene products PagP and PagL, can alter the number of acyl chains in lipid A (reviewed in ref. 4). PagP is a palmitoyl transferase that transfers a palmitoyl moiety from a phospholipid to the *R*-3-hydroxyacyl chain at the 2 position of the glucosamine disaccharide of lipid A (5). PagL hydrolyzes the ester bond at the 3 position of lipid A, thereby releasing the primary 3-OH C14 moiety (6). Both lipid A modifications reduce Toll-like receptor 4 signaling, which could help bacteria to evade the host immune system (7).

PagL was originally identified in *S. typhimurium* (6). Recently, we identified PagL homologs in numerous other Gram-negative bacteria (8). Although the overall sequence conservation was rather low, the enzymatic activity of two of these homologs, including that of *Pseudomonas aeruginosa*, was confirmed because they deacylated *Escherichia coli* LPS. Because *P. aeruginosa* lipid A carries 3-OH C10, rather than 3-OH C14 at the 3 position, these results also demonstrate that the enzyme lacks fatty acyl chain-length specificity. Furthermore, PagL was predicted to form an eight-stranded β-barrel, and Ser-128 and His-126 of *P. aeruginosa* PagL were shown to be essential for activity (8). Here, we present the crystal structure of PagL from *P. aeruginosa* at 2.0-Å resolution and provide insights into the catalytic mechanism and substrate binding of the enzyme.

Results

Production, Folding, and Activity of Recombinant PagL. PagL from *P. aeruginosa* was refolded from inclusion bodies. Folding could be monitored by SDS/PAGE analysis. Like many outer membrane proteins (OMPs), PagL showed heat modifiability (Fig. 1*A*). Usually, the folded form of an OMP has a higher electrophoretic mobility than its denatured form. In the case of PagL, however, the folded protein has a lower electrophoretic mobility as has been observed also for a few other small OMPs, i.e., OmpA171t, OmpX, and NspA (9, 10). The same mobility shift was observed on Western blot for wild-type PagL folded *in vivo* (data not shown). Folded PagL was insensitive to denaturation by SDS, as it remained folded even in the presence of 2% SDS when not heated (Fig. 1*A*).

To verify that PagL was correctly folded *in vitro*, it was incubated with purified LPS of *Neisseria meningitidis* as described in the *Supporting Text*, which is published as supporting information on the PNAS web site. The LPS was converted into a form with a higher electrophoretic mobility (Fig. 1*B*), in agreement with the expected hydrolysis of the primary acyl chain at the 3 position of lipid A, which is 3-OH C12 in the case of *N. meningitidis*. Deacylation of the LPS was confirmed by electrospray ionization mass spectrometry (Fig. 6, which is published as supporting information on the PNAS web site). The reaction was independent of the presence of divalent cations, as deacylation of LPS was still ob-

Conflict of interest statement: No conflicts declared.

This paper was submitted directly (Track II) to the PNAS office.

Abbreviations: OMP, outer membrane protein; MR, molecular replacement; Se-Met, selenomethionine; OMPLA, outer membrane phospholipase A.

Data deposition: The coordinates and structure factors have been deposited in the Protein Data Bank, www.pdb.org (PDB ID code 2ERV).

†L.R. and J.G. contributed equally to this work.

**To whom correspondence should be addressed. E-mail: j.p.m.tommassen@bio.uu.nl.

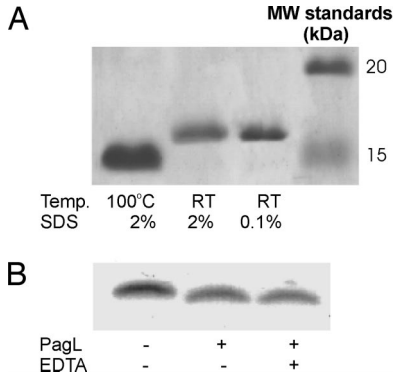

Fig. 1. Folding and *in vitro* activity of recombinant PagL. (*A*) Coomassie-stained SDS/PAGE gel showing the heat modifiability of purified, refolded PagL. Samples were treated in sample buffer containing either 2% or 0.1% SDS and at room temperature (RT) or 100°C before electrophoresis. The positions of molecular mass standard proteins are shown at the right. (*B*) Purified *N. meningitidis* LPS was incubated in a detergent-containing buffer with or without refolded PagL and analyzed by Tricine-SDS/PAGE and staining with silver.

served in the presence of 5 mM EDTA (Fig. 1*B*). Quantification of the amount of 3-OH C12 released in time revealed a specific activity of 0.40 nmol 3-OH C12 released per min per nmol of *in vitro* folded PagL. *E. coli* membranes containing overexpressed *in vivo* folded wild-type PagL displayed a lipid A-deacylase activity of ≈0.22 nmol/min per nmol of PagL, which is comparable to the specific activity of *in vitro* folded PagL. We concluded that PagL was correctly folded *in vitro* into its active conformation and, thus, suitable for structure determination.

Structure Determination of PagL. PagL was crystallized in the C2 space group, containing two molecules in the asymmetric unit (Fig. 7, which is published as supporting information on the PNAS web site). The structure of PagL was solved with a combination of molecular replacement (MR) using the program PHASER (11), together with single-wavelength anomalous dispersion. MR was successfully performed by using a polyalanine model of the β-stranded part of NspA. The calculated $2F_o - F_c$ maps (even after prime-and-switch in RESOLVE, ref. 12) did not allow for initial model tracing by hand or by automated model building with ARP/WARP (13). Determination of the position of the single methionine present in PagL, using the anomalous signal of the selenium from a crystal of selenomethionine (Se-Met)-substituted protein, enabled limited model tracing and subsequent automated model building. The structure was refined to 2.0-Å resolution.

The overall structure of PagL consists of an eight-stranded antiparallel β-barrel, which is consistent with our earlier prediction of its topology (8). So far, the N and C termini of the β-barrel part in all OMP structures solved are facing the periplasm (reviewed in ref. 14). Therefore, we propose that the same holds for PagL. In this orientation, the previously identified active-site residues Ser-128 and His-126 (8) are located near the hydrophilic/hydrophobic boundary of the outer leaflet of the outer membrane (Fig. 2*A*). This position would be consistent with the location of the scissile bond of the substrate LPS. Like other OMPs, PagL has long extracellular loops (L) and short periplasmic turns (T), except for T1, which is exceptionally long (Fig. 2*A*).

Orientation of PagL in the Membrane. Like most other OMPs, PagL contains two girdles of aromatic residues, which are located at the hydrophobic/hydrophilic boundaries of the membrane and are assumed to stabilize the position of the protein in the membrane. Because these girdles are not perpendicular to the β-barrel axis of PagL, as they usually are in OMPs, the orientation of PagL in the membrane may be tilted (Fig. 2*A*). Therefore, we calculated the net hydrophobicity at the β-barrel surface as a function of the height in the membrane as described (15); this was done for two orientations, i.e., with the β-barrel axis parallel or with a 30° tilt angle relative to the membrane normal (Fig. 2*B*). In the tilted orientation, the graph resembles the average graph calculated for all OMP β-barrel structures, in which two hydrophobic peaks represent the aromatic girdles (15). Remarkably, the hydrophobic peak at the extracellular side is much lower than that at the periplasmic side, which can easily be explained by the presence of a highly hydrophilic active site at that height in the barrel (see below). Also, in the parallel orienta-

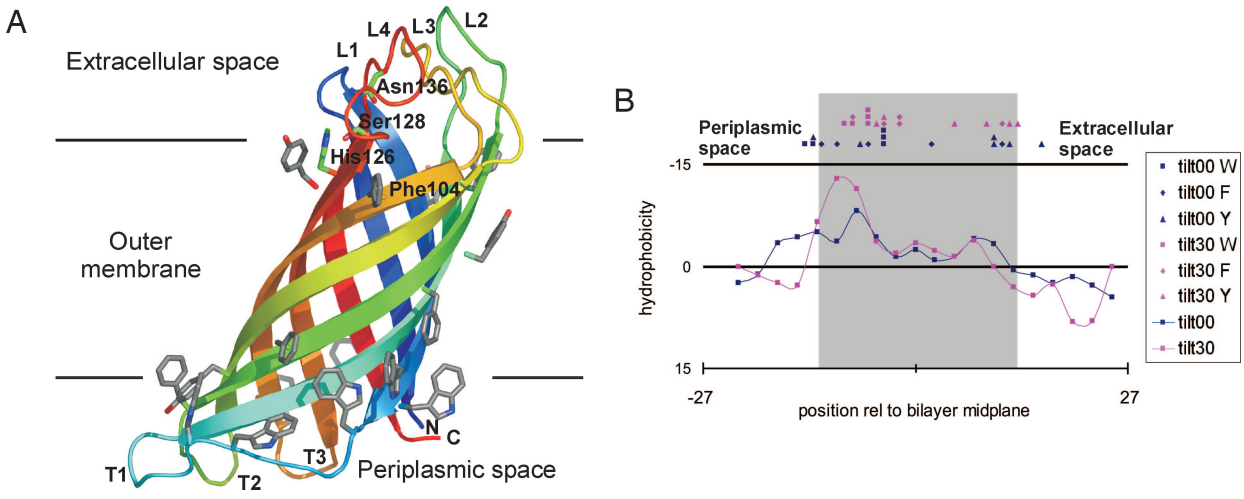

Fig. 2. PagL structure and membrane orientation. (*A*) Ribbon representation of PagL. The N and C termini are labeled and colored blue and red, respectively, with gradient colors in between. The four extracellular loops are labeled L1–L4, and the three periplasmic turns are labeled T1–T3. Aromatic residues located at the presumed membrane boundaries are shown in gray, with nitrogen and oxygen atoms shown in blue and red, respectively. The only four completely conserved residues among PagL homologs are labeled. (*B*) Hydrophobicity profiles for the outward-facing PagL residues as a function of membrane position (periplasmic side left, extracellular side right) are shown as solid lines. Negative Σ(Δ*G*) values indicate regions that are more hydrophobic. The blue line and symbols present results for the positions with the β-barrel axis aligned along the membrane normal, whereas the magenta line and symbols are for the protein tilted by 30°. The symbols represent the Cγ positions of Trp (squares), Tyr (circles), and Phe (triangles) residues that form the inner and outer aromatic girdles. The image shown in *A* was prepared with PYMOL (www.pymol.org).

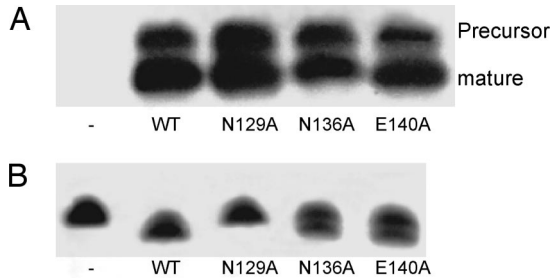

Fig. 3. Identification of residues important for PagL activity. Cells of *E. coli* BL21 Star (DE3) containing the empty pET11a vector, the $pPagL_{(Pa)}$ plasmid, or the mutant $pPagL_{(Pa)}$ plasmids, exponentially growing in LB, were induced with isopropyl β-D-thiogalactoside for 75 min, after which 1-A_{600}-unit culture samples were collected and analyzed by SDS/PAGE followed by immunoblotting with primary antibodies against PagL (*A*) and by Tricine-SDS/PAGE to visualize LPS (*B*). In *A*, the positions of mature PagL and of the precursor form, which accumulated because of overexpression, are indicated.

tion, two hydrophobic peaks can be discriminated. However, the area of hydrophobicity of the intracellular peak extends considerably into the periplasm, suggesting that a parallel orientation is energetically highly unfavorable. Therefore, we propose that PagL has a tilted orientation in the membrane.

PagL Catalytic Mechanism. Previously, we identified PagL homologs in the genomes of a wide variety of Gram-negative bacteria (8). These homologs exhibited a low overall mutual sequence identity, with only 10 conserved residues among 14 different homologs. Here, we performed a more extensive search, which revealed additional PagL homologs in *Caulobacter crescentus*, *Collimonas fungivorans*, *Chlorobium tepidum*, *Rhodospirillum rubrum*, *Sinorhizobium meliloti*, and *Ralstonia eutropha*. An alignment of all currently identified PagL homologs is presented in Fig. 8, which is published as supporting information on the PNAS web site. Among all PagL homologs identified so far, only four amino acid residues are fully conserved, i.e., Phe-104, His-126, Ser-128, and Asn-136 of the *P. aeruginosa* PagL sequence.

Active sites of hydrolases comprise three important regions: the catalytic site, a substrate-binding site, and an oxyanion hole. Classical serine esterases contain a catalytic site consisting of a Ser-His-Asp/Glu triad. The histidine abstracts a proton from the serine residue, after which the serine performs a nucleophilic attack on the carbonyl carbon of the scissile bond. This attack can only be performed efficiently if the Nε2 of the histidine is deprotonated. Deprotonation of the histidine is achieved by stabilization of the proton on the Nδ1 of the histidine via a hydrogen bond with an acidic residue. Usually, this acidic residue is an aspartate or a glutamate. However, in a few exceptions, such as in outer membrane phospholipase A (OMPLA) of *E. coli*, an asparagine residue is also able to stabilize the deprotonated state of the Nε2 of the histidine (16).

Site-directed mutagenesis studies have shown that His-126 and Ser-128 (8) are important for catalytic activity and constitute part of the active site of PagL. In the crystal structure, two acidic residues, Glu-140 and Asp-106, are located in close proximity to His-126. A hydrogen bond is present between the carboxylate of Glu-140 and the Nδ1 hydrogen of His-126, which implies that Glu-140 is the acidic component of the catalytic triad. This notion is supported by the observation that a Glu140Ala substitution reduced the activity of PagL *in vivo* in *E. coli* membranes (Fig. 3). LPS was almost completely converted into its 3-*O*-deacylated form 75 min after induction of expression of wild-type *pagL*, whereas ≈50% remained in the acylated form when the mutant PagL was produced. In the quantitative assay, in which the release of 3-OH C12 from exogeneously added Neisserial LPS is measured, the mutated protein appeared 142-fold less active than the wild type.

Another acidic residue, Asp-106, is present on the opposite side of His-126. In the crystal structure, Asp-106 coordinates a Ca^{2+} ion. Because PagL activity is not influenced by EDTA, this Ca^{2+} ion is likely not relevant for activity and may just be a crystallization artifact. Because Asp-106 points toward the hydrophobic region of the membrane, which is not a favorable position for a charged residue, it seems plausible that it has an important function in the catalytic mechanism. To test this possibility, we substituted Asp-106 by Ala. Unfortunately, the mutant protein was poorly expressed (data not shown), indicating that the substitution caused folding and/or stability problems of the protein.

To gain further insight into the catalytic mechanism, we modeled lipid X, the smallest known substrate of PagL *in vitro* (6) into the active site of PagL by using the program HADDOCK (17). Several restraints were used. The distances between the hydroxyl oxygen of Ser-128 and the carbonyl carbon of the scissile bond and between the Nε2 of His-126 and the main-chain oxygen of the ester bond were both restrained to 3 Å. Furthermore, the acyl chains of lipid X were restrained to point toward the periplasm. In the resulting model (Fig. 4), the residual acyl chain (i.e., the chain to be cleaved off from the substrate) of lipid X is bound in a well defined hydrophobic groove, whereas the acyl chain of the leaving group is loosely bound into a second hydrophobic groove. The conserved residue Phe-104, which makes a hydrophobic interaction with the residual acyl chain, is likely to be a key residue for positioning the substrate into the correct orientation. Furthermore, the hydroxyl

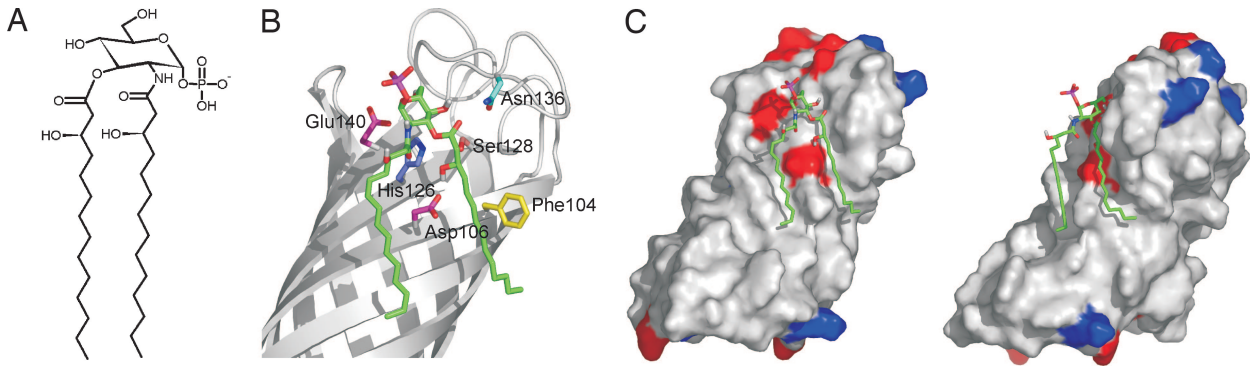

Fig. 4. Modeling of lipid X onto the active site of PagL. (*A*) Schematic representation of lipid X. (*B*) Lipid X modeled onto the active site of PagL. PagL is represented as a gray ribbon diagram. Lipid X is shown as green sticks with oxygen atoms in red and a phosphate atom in magenta. The hydrogen atoms from hydroxyl groups are shown in gray. Some amino acid residues important for PagL activity are shown as sticks and are labeled. (*C*) Two views (≈90° rotated) of the electrostatic surface potential of PagL with lipid X. Positively and negatively charged residues are colored blue and red, respectively. Lipid X is shown as green sticks. The images in *B* and *C* were prepared with PYMOL (www.pymol.org).

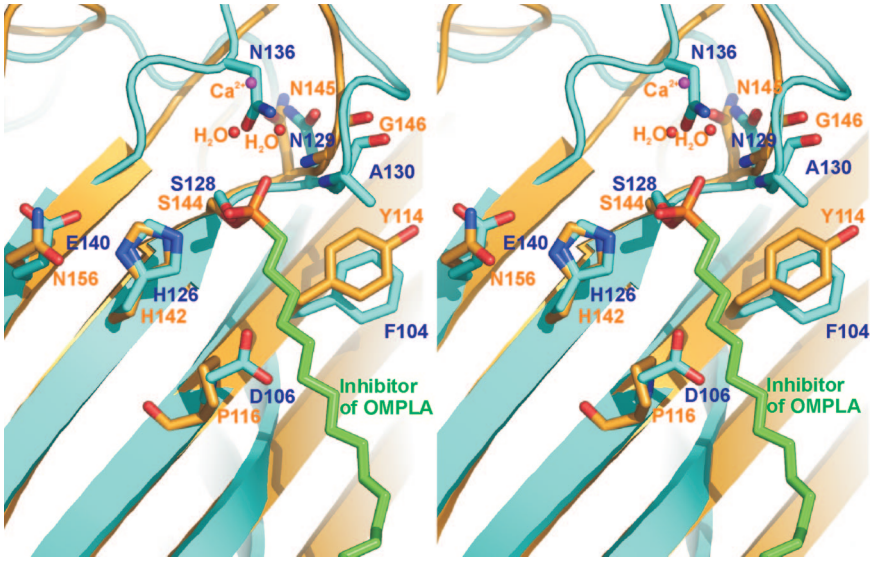

Fig. 5. Stereo diagram of the active site Ser-128 and His-126 of PagL superposed on the active site Ser-144 and His-142 of OMPLA. PagL is shown in cyan, whereas OMPLA is represented in orange. Residues and atoms that may have an important role for activity are shown as sticks and are labeled with cyan and orange text for PagL and OMPLA, respectively. The hexadecanesulfonyl moiety of an OMPLA inhibitor is covalently attached to Ser-144 of OMPLA and colored green. The image was prepared by using PYMOL (www.pymol.org).

group of the residual acyl chain makes a hydrogen bond to Asp-106, suggesting a possible role for this residue in substrate specificity.

The structure of one other outer membrane esterase has been solved, i.e., that of OMPLA, which forms a 12-stranded β-barrel with a catalytic site composed of a Ser-His-Asn catalytic triad (16). To compare the catalytic sites of OMPLA and PagL, we superposed Ser-128 and His-126 of PagL onto Ser-144 and His-142 of OMPLA (Fig. 5). In both PagL and OMPLA, the active sites are located at comparable heights in the barrel relative to the membrane. Furthermore, Glu-140 of PagL occupies the structurally equivalent position of Asn-156, the acidic residue in the catalytic triad of OMPLA, consistent with Glu-140 being the acidic residue of the PagL catalytic triad. In many serine hydrolases, the oxyanion hole consist of two backbone amide groups that form a slightly positively charged center that stabilizes the transient negative charge on the carbonyl oxygen of the substrate during the reaction. The oxyanion hole of OMPLA is formed by two backbone nitrogens from two glycine residues and two water molecules, coordinated by a calcium ion (16). For PagL, the oxyanion hole could well be formed by the two backbone nitrogens of the highly conserved Ala-130 and Gly-131 residues, which are located at the equivalent positions of the oxyanion-hole glycines in OMPLA. Comparison of the OMPLA and PagL active sites further showed that the side-chain nitrogen of Asn-136, the fourth completely conserved residue among the PagL homologs, occupies the position of one of the oxyanion-hole waters in OMPLA (Fig. 5). Therefore, we speculate that the side-chain amide group of Asn-136 is part of the oxyanion hole of PagL. This possibility is supported by the observation that an Asn136Ala mutant derivative of PagL was less active *in vivo* than wild-type PagL (Fig. 3). In the quantitative assay, the activity of this mutant protein was reduced 304-fold. In addition to the three highly or even completely conserved residues Ala-130, Gly-131, and Asn-136, which we postulate to form the oxyanion hole of PagL, one other residue, Asn-129, shows a high conservation among the PagL homologs (see Fig. 8). Furthermore, the same residue is present at the equivalent position in OMPLA (Fig. 5). We propose that Asn-129 of PagL might play a crucial role in stabilizing the conformation of loop 4 and thereby that of the oxyanion hole and the active site. The importance of Asn-129 for the enzymatic activity is supported by the observation that an Asn129Ala mutant derivative of PagL showed no activity *in vivo* (Fig. 3), nor in the quantitative assay even after 27 h incubation with the substrate.

Discussion

The lipid A deacylase PagL was initially discovered in *S. typhimurium*, and, recently, PagL homologs were identified in a wide variety of Gram-negative bacteria, including *P. aeruginosa*. By using these PagL homologs as leads, we were able to identify additional homologs, which now brings their total number to 23. Remarkably, besides the previously identified active-site His and Ser residues, only a Phe and an Asn residue are completely conserved among all homologs identified so far. Modeling with HADDOCK suggested that the phenylalanine is important for positioning the substrate correctly into a hydrophobic groove present on PagL, thereby bringing the scissile bond into close proximity to the active-site serine. This hypothesis is sustained by the presence of another aromatic residue, Tyr-114, at the equivalent position in OMPLA, which was shown to have a similar active-site architecture. This tyrosine was shown to make a hydrophobic interaction in the crystal structure of OMPLA with the substrate analog hexadecanesulfonylfluoride. The close resemblance of the PagL active site to that of OMPLA also allowed us to speculate about the location of the oxyanion hole and the possible role of the completely conserved asparagine (Asn-136) therein.

The catalytic triad of PagL is formed by His-126, Ser-128, and, most likely, Glu-140. The hypothesis that Glu-140, rather than Asp-106, is the third member of the catalytic triad is supported by several lines of evidence. First, Glu-140 is located at the structurally equivalent position of Asn-156, the postulated acidic residue in the catalytic triad of OMPLA. Second, Glu-140 forms a hydrogen bond with His-126. Third, mutagenesis showed that Glu-140 is important for PagL activity, although not essential, because residual activity was detected after its substitution by Ala. In OMPLA, Asn-156 is not essential either, because Asn156Ala substitution reduced OMPLA activity $\approx$20-fold (18). A possible explanation is that OMPLA, and probably also PagL, has a highly functional oxyanion hole that can partly compensate for the loss of the acidic residue. The acidic residue of the catalytic triad of serine hydrolases can be formed by three different amino acids, i.e., Asp, Glu, and, more rarely, Asn. An alignment of all identified PagL homologs (see Fig.

8) shows that always one of these residues is present at the position of Glu-140 in *P. aeruginosa* PagL, except in three cases, i.e., the PagL homologs of *Agrobacterium tumefaciens*, *S. meliloti*, and *R. eutropha*, where a threonine, a threonine, and an alanine, respectively, are present. Theoretically, a threonine could take over the role of the acidic residue in forming a hydrogen bond with the active-site histidine, and it will be interesting to determine by site-directed mutagenesis and x-ray crystallography whether the threonine indeed plays such a role in the *A. tumefaciens* and *S. meliloti* enzymes. The *R. eutropha* enzyme may be less active, like the Glu140Ala-mutant derivative of *P. aeruginosa* PagL, and it will be interesting to determine whether its activity can be enhanced by substituting an acidic residue for the alanine. In the modeled PagL/lipid X structure, the hydroxyl group of the residual acyl chain makes a hydrogen bond to Asp-106. In OMPLA, a proline (Pro-116) is present at the equivalent position. It is tempting to speculate that Asp-106 determines the specificity of PagL for substrates with a hydroxyl group present at the correct position, i.e., for LPS. It will be interesting to determine the consequences of Asp106Pro and Pro116Asp substitutions in PagL and OMPLA, respectively, for the substrate specificity of the enzymes. It should be noted, however, that Asp-106 is not completely conserved among all PagL homologs, and one enzyme, i.e., that of *C. crescentus*, contains a proline at the equivalent position (see Fig. 8).

Taken together, monomeric PagL has all features needed for activity, i.e., an active site, an oxyanion hole, and a substrate-binding pocket within a single molecule. In contrast, OMPLA activity is activated *in vitro* by dimerization (16). This raises the question in what way enzymatic activity of PagL is controlled. In *S. typhimurium*, expression of *pagL* is under the control of the PhoP/PhoQ two-component regulatory system. However, silencing of PagL activity, when it is no longer beneficial to the bacterium, is not explained. A recent observation may provide an answer: PagL of *S. typhimurium* is inhibited by modification of LPS with aminoarabinose (19). It was suggested that such modification might affect the membrane localization or conformation of PagL. However, in *P. aeruginosa*, modification of LPS with aminoarabinose is found in combination with 3-*O*-deacylation of lipid A, suggesting that PagL activity is not regulated in this way in *P. aeruginosa* (20). In contrast to the activation caused by dimerization of OMPLA, dimerization of PagL could inhibit PagL activity. The active sites of the two PagL molecules in the asymmetric unit are in close proximity (see Fig. 7). It is tempting to speculate that this structure represents a dimeric state of PagL. After substitution of the active-site serine by a cysteine, we detected dimers of the protein when the membranes were analyzed by SDS/PAGE in the absence of a reducing agent (data not shown), indicating that the active sites of the two PagL molecules could be very close *in vivo* as well. If indeed such a dimer is formed, the active site of one monomer is shielded for substrate binding by the other monomer. Therefore, dimerization may be an inactivation mechanism for PagL, whereas it is an activation mechanism in the case of OMPLA.

Both the length of turn T1 and the position of the aromatic residues raised the idea that the PagL β-barrel is tilted relative to the membrane plane. Interestingly, such an assumption has been made for only one other OMP, i.e., the lipid A-modifying enzyme PagP (21). Analysis of the hydrophobic surface of the β-barrel indeed showed that a tilted orientation of PagL is more consistent with the average hydrophobicity profile of other β-barrels of known structure. The tilted orientation also explains why the periplasmic turn (T1) between strands 2 and 3 is asymmetrical and contains many aromatic residues. Considering the hydrophobicity profiles of possible orientations tested, a 30°-tilted orientation is expected to be energetically most favorable. However, in a biological membrane, there are many more forces and factors that determine the position of a protein. The shape of the LPS and phospholipids and the lateral pressure exerted by these will form a counterbalancing force against tilting of the barrel. Therefore, it cannot be concluded that PagL has a 30° tilt *in vivo*, although such an angle might be considered as the maximal possible tilt. Furthermore, control of the barrel tilt angle and, thereby, of the position of the active site relative to the membrane might form another mechanism to control the enzymatic activity of PagL *in vivo*.

LPS is known for its endotoxic activity when administered to higher organisms. This endotoxic activity is responsible for the side effects that are often seen when vaccines that contain LPS are administered. LPS also has a powerful adjuvant activity. Unfortunately, a broad-scale use of this adjuvant quality is not possible because of the endotoxic activity. Recently, it has been shown that changing the physico-chemical properties of LPS influences its endotoxic activity (1, 22, 23). Thus, LPS-modifying enzymes may be valuable tools for detoxification of LPS. We showed here that purified and *in vitro* refolded PagL is active against externally added LPS. Thus, *in vitro* refolded PagL might be used for the detoxification of LPS *in vitro* and thereby be useful for the development of new vaccines or adjuvants. Furthermore, the structure of PagL may form, especially because the active site is on the outside of the barrel, a basis for the design of inhibitors with possible therapeutic value.

Materials and Methods

Site-Directed Mutagenesis. Mutations were introduced in *pagL* by using the QuikChange Site-Directed Mutagenesis kit (Stratagene) and the primers listed in Table 2, which is published as supporting information on the PNAS web site. Plasmid $pPagL_{(Pa)}$ encoding wild-type PagL, including the signal sequence (8), was used as the template in which the mutations were created. The presence of the correct mutations was confirmed by nucleotide sequencing in both directions.

***In Vitro* Folding of PagL.** PagL was produced in *E. coli* as described in *Supporting Text* and folded *in vitro* by 2-fold dilution from a stock solution in 8 M urea into 10% (wt/vol) lauryldimethylamine-oxide, followed by 10 min of sonication using a Branson 1210 Sonifier. Refolded PagL was diluted 3- to 4-fold with buffer A [20 mM Tris·HCl, pH 8.5/0.08% (wt/vol) pentaethyleneglycol monodecyl ether ($C_{10}E_5$)] and purified by FPLC using a 1-ml monoQ (Amersham Pharmacia) ion-exchange column that was preequilibrated with buffer A. PagL was eluted with a linear gradient of 0–1 M NaCl in buffer A. Fractions containing PagL were pooled and concentrated to ≈10 mg/ml by using Centricon concentrators with a molecular mass cutoff of 3 kDa (Amicon). The protein was then dialyzed three times overnight against 10 ml of 2 mM Tris·HCl, pH 8.5/0.06% (vol/vol) $C_{10}E_5$ using a membrane with a molecular mass cutoff of 3.5 kDa.

Crystallization and Structure Determination. PagL was crystallized by using the hanging-drop vapor diffusion method. Crystals grew in the C2 space group, using a condition containing 3% PEG3000/25% glycerol/10 mM calcium acetate/0.1 M Tris·HCl, pH 8.5 at 20°C. Se-Met PagL crystals were grown in the same condition, with 1 mM DTT added to the protein solution. Crystals were harvested from the drops with a cryo-loop and directly cooled into liquid nitrogen. Data sets were obtained at 100 K on a charge-coupled device detector at beamline ID14-EH4 at the European Synchrotron Radiation Facility. Native data were collected to 2.0-Å resolution. Data of the Se-Met PagL crystal was collected at λ_{peak} = 0.9795 to 2.8-Å resolution. All data were indexed and processed by using DENZO and SCALEPACK (24). Table 1 summarizes data collection information. The structure of PagL was solved by using a combination of Se-Met single-wavelength anomalous dispersion (SAD) and MR. From the Se-Met SAD data set, the two selenium atoms in the asymmetric unit (one per PagL molecule) were located by using standard programs (12, 25, 26). Unfortunately, the anomalous signal was too low to obtain an interpretable density-modified electron-density map. Therefore, we attempted MR. Whereas all

Table 1. Data collection and refinement statistics

	Native	Se-Met
Data collection		
Space group	C2	C2
Cell dimensions		
a, Å	92.26	93.21
b, Å	48.99	47.66
c, Å	105.03	103.45
β, °	115.46	113.39
Resolution, Å (outer shell)	2.00 (2.05)	2.80 (2.87)
R_{sym} or R_{merge}	0.051 (0.380)	0.098 (0.515)
$I/\sigma I$	20.9 (3.0)	19.3 (3.4)
Completeness, %	90.3 (52.2)	99.8 (97.6)
Redundancy	3.1 (2.7)	6.8 (6.9)
Refinement		
Resolution, Å	2.00	
No. of reflections	26,283	
R_{work}/R_{free}	0.198/0.233	
No. of atoms	2,518	
Protein	2	
Ligand/ion	12 ($C_{10}E_5$ parts)/1 (Ca^{2+})	
Water	121	
B factors		
Protein	29.40	
Ligand/ion	50.22/22.41	
Water	39.97	
rms deviations		
Bond lengths, Å	0.017	
Bond angles, °	1.657	

commonly used MR programs failed, the program PHASER (11) provided an MR solution using a polyalanine β-barrel model of the NspA structure, lacking the loops. The poor phases obtained from the incomplete model were sharpened by using the prime-and-switch algorithm in the program SOLVE (12). The positions of the seleniums indicated the locations of the methionines, which enabled us to correctly build a few β-strands by using the program O (27). Subsequently, the complete model could be built automatically by using ARP/WARP (28), which was not the case directly after MR. The structure was refined by using REFMAC 5.0 (29), using TLS groups for the separate molecules in the asymmetric unit. Refinement statistics are summarized in Table 1, and the electron density map is shown in Fig. 9, which is published as supporting information on the PNAS web site.

Modeling of Lipid X onto the Active Site of PagL. Models of lipid X docked onto PagL were created by using the program HADDOCK (17). The coordinates of PagL were taken from chain A of the structure and the lipid X coordinates were based on those of the LPS molecule that was cocrystallized with FhuA (30). Ambiguous interaction restraints (AIRs) were defined, based on the information on the reaction mechanism: 3-Å-distance restraints were defined between the Ser-128 oxygen of PagL and the carboxyl carbon of lipid X and between the His-126 nitrogen (Nε2) and the ester oxygen of lipid X. Additional AIRs were imposed merely to ensure that the lipid X acyl chains were positioned at least as close to the PagL molecule as they could be in the outer leaflet of the outer membrane. First, an ensemble of 20 conformations of lipid X was generated by simulated annealing and molecular dynamics refinement in DMSO, which was subsequently used to generate 1,000 rigid body docking solutions. The best 200 solutions based on their intermolecular energy (sum of van der Waals, electrostatic, and AIR energies) were then submitted to a semiflexible refinement, during which lipid X was treated as fully flexible, whereas PagL could only move at defined flexible regions (side chains first, subsequently both side chains and backbone). All 200 models were finally refined in explicit solvent (DMSO was used to mimic the hydrophobic environment imposed by the membrane) and clustered based on root mean square deviation criteria. The lowest energy structure from the lowest energy cluster was taken as best solution.

We are grateful for measurement time at the beam line ID14-EH4 at the European Synchrotron Radiation Facility in Grenoble. This work was supported by the council for Chemical Sciences of the Netherlands Organization for Scientific Research (NWO-CW).

1. Raetz, C. R. & Whitfield, C. (2002) *Annu. Rev. Biochem.* **71,** 635–700.
2. Miyake, K. (2004) *Trends Microbiol.* **12,** 186–192.
3. Bader, M. W., Sanowar, S., Daley, M. E., Schneider, A. R., Cho, U., Xu, W., Klevit, R. E., Le Moual, H. & Miller, S. I. (2005) *Cell* **122,** 461–472.
4. Trent, M. S. (2004) *Biochem. Cell Biol.* **82,** 71–86.
5. Bishop, R. E., Gibbons, H. S., Guina, T., Trent, M. S., Miller, S. I. & Raetz, C. R. (2000) *EMBO J.* **19,** 5071–5080.
6. Trent, M. S., Pabich, W., Raetz, C. R. & Miller, S. I. (2001) *J. Biol. Chem.* **276,** 9083–9092.
7. Kawasaki, K., Ernst, R. K. & Miller, S. I. (2004) *J. Biol. Chem.* **279,** 20044–20048.
8. Geurtsen, J., Steeghs, L., Hove, J. T., van der Ley, P. & Tommassen, J. (2005) *J. Biol. Chem.* **280,** 8248–8259.
9. Pautsch, A., Vogt, J., Model, K., Siebold, C. & Schulz, G. E. (1999) *Proteins* **34,** 167–172.
10. Vandeputte-Rutten, L., Bos, M. P., Tommassen, J. & Gros, P. (2003) *J. Biol. Chem.* **278,** 24825–24830.
11. Storoni, L. C., McCoy, A. J. & Read, R. J. (2004) *Acta Crystallogr. D* **60,** 432–438.
12. Terwilliger, T. C. (2003) *Methods Enzymol.* **374,** 22–37.
13. Perrakis, A., Sixma, T. K., Wilson, K. S. & Lamzin, V. S. (1997) *Acta Crystallogr. D* **53,** 448–455.
14. Schulz, G. E. (2000) *Curr. Opin. Struct. Biol.* **10,** 443–447.
15. Wimley, W. C. (2002) *Protein Sci.* **11,** 301–312.
16. Snijder, H. J., Ubarretxena-Belandia, I., Blaauw, M., Kalk, K. H., Verheij, H. M., Egmond, M. R., Dekker, N. & Dijkstra, B. W. (1999) *Nature* **401,** 717–721.
17. Dominguez, C., Boelens, R. & Bonvin, A. M. (2003) *J. Am. Chem. Soc.* **125,** 1731–1737.
18. Kingma, R. L., Fragiathaki, M., Snijder, H. J., Dijkstra, B. W., Verheij, H. M., Dekker, N. & Egmond, M. R. (2000) *Biochemistry* **39,** 10017–10022.
19. Kawasaki, K., Ernst, R. K. & Miller, S. I. (2005) *J. Bacteriol.* **187,** 2448–2457.
20. Ernst, R. K., Yi, E. C., Guo, L., Lim, K. B., Burns, J. L., Hackett, M. & Miller, S. I. (1999) *Science* **286,** 1561–1565.
21. Ahn, V. E., Lo, E. I., Engel, C. K., Chen, L., Hwang, P. M., Kay, L. E., Bishop, R. E. & Prive, G. G. (2004) *EMBO J.* **23,** 2931–2941.
22. Loppnow, H., Brade, H., Durrbaum, I., Dinarello, C. A., Kusumoto, S., Rietschel, E. T. & Flad, H. D. (1989) *J. Immunol.* **142,** 3229–3238.
23. Steeghs, L., Berns, M., ten Hove, J., de Jong, A., Roholl, P., van Alphen, L., Tommassen, J. & van der Ley, P. (2002) *Cell Microbiol.* **4,** 599–611.
24. Otwinowski, Z. & Minor, W. (1997) *Methods Enzymol. A* **276,** 307–326.
25. Weeks, C. M. & Miller, R. (1999) *Acta Crystallogr. D* **55,** 492–500.
26. Schneider, T. R. & Sheldrick, G. M. (2002) *Acta Crystallogr. D* **58,** 1772–1779.
27. Jones, T. A., Zou, J. Y., Cowan, S. W. & Kjeldgaard (1991) *Acta Crystallogr. A* **47,** 110–119.
28. Perrakis, A., Harkiolaki, M., Wilson, K. S. & Lamzin, V. S. (2001) *Acta Crystallogr. D* **57,** 1445–1450.
29. Winn, M. D., Isupov, M. N. & Murshudov, G. N. (2001) *Acta Crystallogr. D* **57,** 122–133.
30. Ferguson, A. D., Hofmann, E., Coulton, J. W., Diederichs, K. & Welte, W. (1998) *Science* **282,** 2215–2220.